



Contents lists available at ScienceDirect

Journal of Wind Engineering and Industrial Aerodynamics

journal homepage: www.elsevier.com/locate/jweia

Hurricane hazard modeling: The past, present, and future

Peter J. Vickery^{a,*}, Forrest J. Masters^b, Mark D. Powell^c, Dhiraj Wadhera^a^a Applied Research Associates, Inc., Raleigh, NC, USA^b University of Florida, Gainesville, FL, USA^c NOAA Hurricane Research Division, Miami, FL, USA

ARTICLE INFO

Article history:

Accepted 18 May 2009

Keywords:

Hurricane
Wind
Risk
Hazard
Gust factor
Boundary layer

ABSTRACT

Hurricane hazard modeling has become a commonly used tool for assessing hurricane risk. The type of hurricane risk considered varies with the user and can be an economic risk, as in the case of the insurance and banking industries, a wind exceedance risk, a flood risk, etc. The most common uses for hurricane hazard models today include:

- (i) Simulation of wind speed and direction for use with wind tunnel test data to estimate wind loads vs. return period for design of structural systems and cladding.
- (ii) Estimation of design wind speeds for use in buildings codes and standards.
- (iii) Coastal hazard risk modeling (e.g. storm surge elevations and wave heights vs. return period).
- (iv) Insurance loss estimation (e.g. probable maximum losses, average annual losses).

This paper presents an overview of the past and present work in hurricane modeling. The wind model is the key input to each of the examples presented above and is the focus herein. We discuss the evolution and current state of wind field modeling, modeling uncertainties, and possible future directions of the hurricane risk modeling process.

© 2009 Elsevier Ltd. All rights reserved.

1. Background

The mathematical simulation of hurricanes is a widely accepted approach for estimating wind speeds for the design of structures and assessment of hurricane risk. The simulation approach is used in the development of the design wind speed maps in the US (ANSI A58.1, 1982; ASCE 7-93 (ASCE, 1993) through to ASCE 7-05 (ASCE, 2006)), the Caribbean (CUBIC, 1985), and Australia (AS/NZS1170.2, 2002). The approach is routinely used in the banking and insurance industries for setting insurance rates. Wind field simulation also drives storm surge models that are used to develop coastal flood estimates and to set flood insurance rates and minimum floor elevations for buildings along the hurricane coastline of the US. Virtually all buildings and bridges that have been wind tunnel tested and are to be built in hurricane and typhoon areas, have had the wind tunnel test data combined in some fashion with the results of a hurricane hazard model. As modern design practice continues to push the requirements of infrastructure performance in hazard prone regions, the need for accurate risk-based engineering analysis has become a critical component. Hurricane simulation has evolved with this need.

The modeling approach has improved significantly since the pioneering studies performed in the late 1960s and early 1970s (e.g. Russell, 1968, 1971; Tryggvason et al., 1976). In principal, the fundamental concept has not changed since the original work of Russell in 1968, but the details have changed, particularly in the modeling of the hurricane wind field. The improvements have come about through the use of more sophisticated physical models. Increased computing capacity has contributed to this effort, but to a large extent the most significant model improvements are due to the enormous increase in quantity and quality of measured data available now to improve and validate the physical and statistical models used to represent the hurricane hazard. This paper discusses the probabilistic and physical models used in the modeling process, examining the changes and improvements to the various components, and proposes expectations for the next generation of hazard models.

2. Probabilistic models

2.1. Single site probabilistic models

The simulation approach was first described in the literature by Russell (1968, 1971). Since then others have expanded and improved the modeling technique in Russell's pioneering study

* Corresponding author.

E-mail address: pjvickery@ara.com (P.J. Vickery).

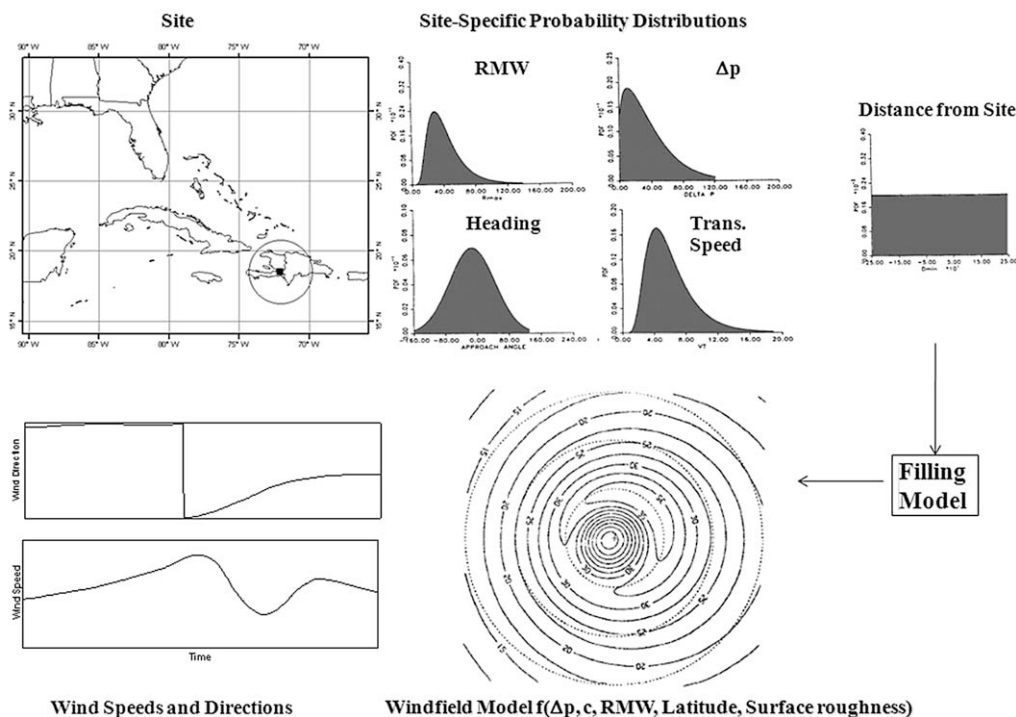


Fig. 1. Overview of simulation modeling approach (site specific modeling).

for US applications, including Tryggvason et al. (1976), Batts et al. (1980), Georgiou et al. (1983), Georgiou (1985), Neumann (1991), and Vickery and Twisdale (1995a). The basic approach used in all of these studies is similar in that site specific statistics of key hurricane parameters are first obtained, including central pressure deficit, radius to maximum winds (RMW), heading, translation speed, and the coast crossing position or distance of closest approach. Given the statistical distributions of these hurricane parameters, a Monte Carlo approach is used to sample from each distribution, and a mathematical representation of a hurricane is passed along the straight line path satisfying the sampled data while the simulated wind speeds are recorded. The intensity of the hurricane is held constant until landfall is achieved, after which the hurricane is decayed using a filling rate model (e.g. DeMaria et al., 2006). The overall simulation methodology is illustrated in Fig. 1. This approach is valid for a single site or small regions only since the required statistics have been developed using site specific data, centered on the sample circle or coastline segments.

The applications of this concept in the previously noted studies are similar, with the major differences being associated with the physical models used, including the filling rate models and wind field models. Other differences include the size of the region over which the hurricane climatology (statistical distributions) can be considered valid, and the use of a coast segment crossing approach (e.g. Russell, 1971; Batts et al., 1980; Tryggvason et al., 1976), or a circular sub-region approach (e.g. Georgiou et al., 1983; Georgiou, 1985; Neumann, 1991; Vickery and Twisdale, 1995a). The studies also differ in the choice of probability distribution to fit a given parameter, such as central pressure (or central pressure difference), RMW, translation speed, etc. The risk model developed by Neumann (1991) differs from the other models in that instead of modeling the central pressure within a hurricane, he modeled the maximum surface wind speed in the hurricane, as defined by the HURDAT database (Jarvinen et al., 1984).

The Batts et al. (1980) model was used to develop the design wind speeds along the hurricane prone coastline of the US, while

the model described by Tryggvason et al. (1976), was likely the first attempt to couple wind tunnel data with simulated hurricane wind speeds to develop design wind loads for individual buildings. None of the works described in Russell (1968), Tryggvason et al. (1976), or Batts et al. (1980), included an attempt to verify that the simple wind field models used in the simulations were able to reasonably reproduce the wind speeds and directions in historical hurricanes. Georgiou (1985) was probably the first to attempt such a wind field model validation.

Darling (1991) formulated a slightly different approach to modeling the hurricane risk. Instead of developing statistical distributions for the central pressure, he developed distributions for the relative intensity of a hurricane and applied his model to hurricane risk in the Miami, Florida area. The relative intensity is a measure of the intensity of a storm (as defined by wind speed or central pressure) compared to the theoretical maximum potential intensity (MPI) of the storm (as defined by wind speed or central pressure). The MPI used by Darling (1991) is defined in Emanuel (1988). A key advantage associated with the introduction of the MPI into the simulation process was that it eliminated (at least for South Florida),¹ the need to artificially truncate the distribution of central pressure, as the MPI imposed a physical limit associated with the minimum central pressure of a simulated storm.

2.2. Hurricane track modeling

Vickery et al. (2000b) published the first technique for modeling the tracks of tropical cyclones. In their track model they incorporated the relative intensity technique pioneered by Darling (1991). The major contribution of Vickery et al. (2000a) track modeling study was the ability to model the hurricane risk

¹ Relative intensities greater than one are possible in the case of intense fast moving storms that track over cold waters, and therefore have intensities greater than the theoretical maximum.

along the coastline of an entire continent, rather than being limited to a single point or a small region. Vickery et al. (2000a) also introduced an additional non-deterministic simulation parameter to the modeling approach with the inclusion of the Holland B parameter (Holland, 1980) as a random variable. This track modeling approach has since been expanded upon by Powell et al. (2005), Hall and Jewson (2005, 2008), James and Mason (2005), Emanuel et al. (2006), Lee and Rosowsky (2007), and proprietary insurance loss modeling companies. The track model developed by Emanuel et al. (2006) combined a stochastic track model with a deterministic axi-symmetric balance model and a 1-D ocean mixing model to model the life cycle of a hurricane. The axi-symmetric balance model used by Emanuel et al. (2006) is described in detail in Emanuel et al. (2004). Given information on sea surface temperature (SST), tropopause temperature, humidity and other parameters, coupled with a training set of historical storms, the model is able to mimic the strengthening and weakening of hurricanes as they progress along the modeled tracks, taking into account the effects of wind shear and ocean mixing, without using statistical models to model the changes in hurricane intensity. One of the key differences between the model developed by Emanuel et al. (2006) and those of Vickery et al. (2000a, 2000b) and Powell et al. (2005), is that Emanuel et al. (2006) model is “calibrated” to match National Hurricane Center estimates of sustained (maximum 1 min average) wind speeds rather than central pressures. The impact of this key difference is discussed later. Vickery et al. (2009a) developed a hybrid model that combines some of the features of Emanuel et al. (2006) model and Vickery et al. (2000a, 2000b) model.

The track modeling approach represents the current state-of-the-art in hurricane risk assessment. It is the stepping stone for the next advancement, pioneered by Emanuel, whereby the track models are coupled with more advanced fully dynamic 3-D numerical weather prediction (NWP) models such as an MM5 (Warner et al., 1978) or a WRF (Skamarock et al., 2008) type model. Whether the introduction of advanced numerical models will reduce the overall uncertainty in the track modeling process, caused primarily by the limited data associated with the historical record of hurricanes, remains to be seen.

3. Hurricane wind field modeling

Wind field modeling is a three step process:

- (1) Given key input values (central pressure, RMW, etc.) an estimate of the wind speed at gradient height is obtained. It is assumed to be equivalent to a mean wind speed.
- (2) This gradient wind speed is adjusted to a mean surface wind speed value at a specified height using atmospheric boundary layer (BL) concepts assuming neutral stability.
- (3) The mean surface wind speed is adjusted for terrain and averaging time using gust factors. The evolution and current state of each of these three steps is discussed next.

3.1. Gradient wind field modeling

The sophistication of the gradient wind field models applied in the hazard simulation models has improved significantly since the 1970s, and continues to improve. In Batts et al. (1980) model, the maximum gradient wind speed is modeled as

$$V_{G \max} = K \sqrt{\Delta p - \frac{RMWf}{2}} \approx K \sqrt{\Delta p} \quad (1)$$

where K is an empirical constant, Δp the central pressure difference, defined as the difference between the pressure at the

center of the storm and the far field pressure, normally taken as the pressure associated with the first anticyclonically curved isobar, RMW the radius to maximum winds, and f the Coriolis parameter. The variation of the wind speed away from the maximum was described using a nomograph. Similar simple models were used in Russell (1968) and Schwerdt et al. (1979). The maximum gradient wind speed in the model used (Tryggvason et al., 1976) was also proportional to $\sqrt{\Delta p}$ but used an analytic representation of the entire wind field rather than using a nomograph approach as in Batts et al. (1980).

Holland (1980) introduced a representation of the gradient hurricane wind field that has been employed in many hurricane risk studies (e.g. Georgiou et al., 1983; Harper, 1999; Lee and Rosowsky, 2007). Holland introduced an additional parameter to define the maximum wind speed in a hurricane, now commonly referred to as the Holland B parameter. The pressure, $p(r)$, at a distance r from the center of the storm is given as

$$p(r) = p_c + \Delta p \exp \left[- \left(\frac{RMW}{r} \right)^B \right] \quad (2)$$

where p_c is the pressure at the center of the storm.

The gradient balance velocity, V_G , for a stationary storm is thus

$$V_G = \left[\left(\frac{RMW}{r} \right)^B B \Delta p \exp \left[- \left(\frac{RMW}{r} \right)^B \right] \frac{1}{\rho} + \frac{r^2 f^2}{4} \right]^{1/2} \frac{f * r}{2} \quad (3)$$

where ρ is the density of air. The maximum wind speed at the RMW is

$$V_{G \max} \approx \sqrt{\frac{B \Delta p}{e \rho}} \quad (4)$$

and thus the maximum velocity in the hurricane is directly proportional $\sqrt{B \Delta p}$ rather than simply being proportional to $\sqrt{\Delta p}$ alone as in most other models.

Georgiou (1985) was the first to use a numerical model of the hurricane wind field for use in risk assessment when he employed the model described in Shapiro (1983), coupled with the Holland model to define the wind speeds at gradient height. In Georgiou's implementation of the Holland model, he constrained B to have a value of unity. Vickery et al. (2000a) also used a numerical model to define the hurricane wind field model, employing a model similar to that of Thompson and Cardone (1996), and driving the model with the pressure field as described in (2), but not constraining B to be equal to 1. The models used by both Georgiou (1985) and Vickery et al. (2000a) were 2-D slab models, and in both cases techniques were implemented in such a way that they used pre-computed solutions to the equations of motion of a translating hurricane in the simulation process. A 2-D numerical model provides a means to take into account the effect of surface friction on wind field asymmetries, enables the prediction of super gradient winds, and models the effect of the sea-land interface (caused by changes in the surface friction) as well as the enhanced inflow caused by surface friction. Three dimensional numerical models potentially provide a means to better model the effect of surface roughness variations on changes in the vertical structure of the hurricane boundary layer, including changes in the boundary layer height, and are capable of simulating localized convective dynamics such as boundary layer roll formation (e.g. Foster, 2005).

Three dimensional models have not appeared in any peer-reviewed published hurricane risk studies so far. However, with the advances in computing power it is highly probable that such models may be used in the future. The use of 3-D models does not

eliminate the need for extensive validation through comparisons with surface level anemometer data, and if the development of observational technologies keeps pace with the 3-D models, validation may evolve to four dimensional variational analysis (4DVAR) that incorporates surfaces observations and the remotely sensed data from ground-, aircraft-, and satellite-based weather observing platforms.

In all of the above noted examples, the estimated gradient wind speed is associated with a long period averaging time of the order of 10 min to an hour. In each of the gradient-level wind field models discussed, the pressure field driving the wind field is assumed to be axi-symmetric, which can be a significant oversimplification.

3.2. Hurricane boundary layer, sea–land transition, and hurricane gust factors

Given an estimate of the mean wind speed at gradient height (V_G), this wind speed is then adjusted to the surface (10 m above water or ground, V_{10}) through the use of an atmospheric boundary layer model or a wind speed reduction factor V_{10}/V_G . The simple reduction factors for winds over the ocean used in the past (and to some extent, still used today) vary from as high as 0.950 (Schwerdt et al., 1979) to a low of about 0.650 (Sparks and Huang, 2001). A value of 0.865 was used by Batts et al. (1980) and Georgiou (1985), used a value of 0.825 near the eyewall, reducing to 0.750 away from the eyewall.

The wind speed ratios for the overland cases associated with the above four studies are 0.845 at the coastline reducing to 0.745, 19 km inland (Schwerdt et al., 1979), 0.450 (Sparks and Huang, 2001), 0.620 (Georgiou, 1985), and 0.740 (Batts et al., 1980). These wind speed ratios correspond to reductions in the mean wind speed, as the wind moves from sea-to-land, of an immediate 11–22% reduction (Schwerdt et al., 1979), 30% reduction (Sparks, 2003), 16–25% reduction over 50 km (Georgiou, 1985), and a 15% reduction (Batts et al., 1980). In Batts et al. (1980), the roughness of the land is characterized by a surface roughness length of 0.005 m. In Sparks and Huang (2001), open terrain is implied as they state that the 0.45 ratio applies to an airport location a few km inland. The Georgiou (1985) wind speed reduction is also applicable to open terrain. In Schwerdt et al. (1979), no reference is given to the land roughness other than to state it is not rough.

Vickery et al. (2000a), modeled the V_{10}/V_G ratio using a hurricane boundary layer model based on Monin–Obukov similarity theory, coupled with an ocean drag coefficient model with the drag coefficient C_d linearly increasing with wind yielding wind speed ratios that varied with both wind speed and the air–sea temperature difference. The Vickery et al. (2000a) study introduced an empirical increase in the wind speed ratio of 10% near the eyewall. For relatively intense storms with an air–sea temperature difference of zero, near the eyewall the typical ratios of V_{10}/V_G were in the range of 0.70–0.72. The reduction in the wind speed as the wind moves from the sea to the land is wind speed dependent because of the use of an un-capped² drag coefficient model to estimate the ocean surface roughness, which was then coupled with ESDU (1982, 1983) wind speed transition models to estimate the mean wind speed in open terrain. The resulting reduction in the mean wind speed varied from ~14% for intense storms to as much as ~20% for weaker storms.

Powell et al. (2005) modeled the mean surface wind speed as equal to 80% of the boundary layer average wind speed, yielding

Table 1

Example model values of V_{10}/V_G and sea–land wind speed reductions.

Source	V_{10}/V_G over water (near eyewall)	Sea–land transition (% reduction of mean wind speed at 10 m)
Schwerdt et al. (1979)	0.95 (PMH) 0.90 (SPH)	11%, at coast 22%, 19 km inland
Batts et al. (1980)	0.865	15%, at the coast
Georgiou (1985)	0.825 $r < 2RMW$ 0.75 $r > 5RMW$	0%, at coast 25%, 50 km inland
Vickery et al. (2000a, 2000b)	~0.70–0.72	14–20%, at the coast 23–28%, 50 km inland
Sparks and Huang (2001)	0.65	30%, a few km inland
Powell et al. (2005)	~0.73	15–20%, at the coast
Powell et al. (2003)	~0.71	N/A
Vickery et al. (2009b)	~0.71 (varies from 0.67 to 0.74)	18–20%, at the coast

$V_{10}/V_G \approx 0.73$, but varying with wind speed. The most recent version of Powell et al. (2005) model has been updated to use a 78% factor instead of an 80% factor. In their transition from sea-to-land, Powell et al. (2005), used an un-capped drag coefficient model³ to estimate the over water surface roughness, and then used the terrain transition model described in Simiu and Scanlan (1996) to compute the reduced over land mean wind speeds, yielding reductions in the mean wind speed similar to those estimated by Vickery et al. (2000a). A summary of the values of V_{10}/V_G for a sample of hurricane “boundary layer” models available in the literature is given in Table 1.

Analysis of dropsonde data collected from 1997 through to the present has improved our understanding of the overall characteristics of the hurricane marine boundary layer, but has also raised new questions. The analysis of Powell et al. (2003) revealed the following:

- The marine boundary layer is logarithmic over the lower ~200 m.
- The mean wind speed at a height of 10 m is equal to ~78% of the mean boundary layer wind speed (average wind over the lower 500 m).
- The mean wind speed at 10 m is equal to ~71% of the maximum (or gradient) wind speed.
- The sea surface drag coefficient increases with wind speed up to a mean wind speed (at 10 m) of about 40 m/s, after which the drag coefficient levels off or perhaps even decreases with increasing wind speed.
- The boundary layer height decreases with increasing wind speed.

Vickery et al. (2009b) also examined the dropsonde data, separating the data by storm size as well as wind speed and coupled their analysis of the dropsonde data with a simplified version of the linearized hurricane model developed by Kepert (2001). In agreement with Kepert (2001), the data showed that the boundary layer height decreases with increasing inertial stability. In agreement with Powell et al. (2003), the data showed the boundary layer is logarithmic over the lower 200–300 m. Fig. 2 shows the variation of mean wind speed with height derived from the analysis of dropsondes for a range of mean boundary layer wind speeds and storm radii as given in

² Prior to Powell et al. (2003), it was incorrectly theorized that the wind speed dependent surface drag coefficient was “un-capped” or that it continued to increase monotonically in >40 m/s winds.

³ A capped representation of the marine drag coefficient was implemented after the 2005 publication (Powell, 2007).

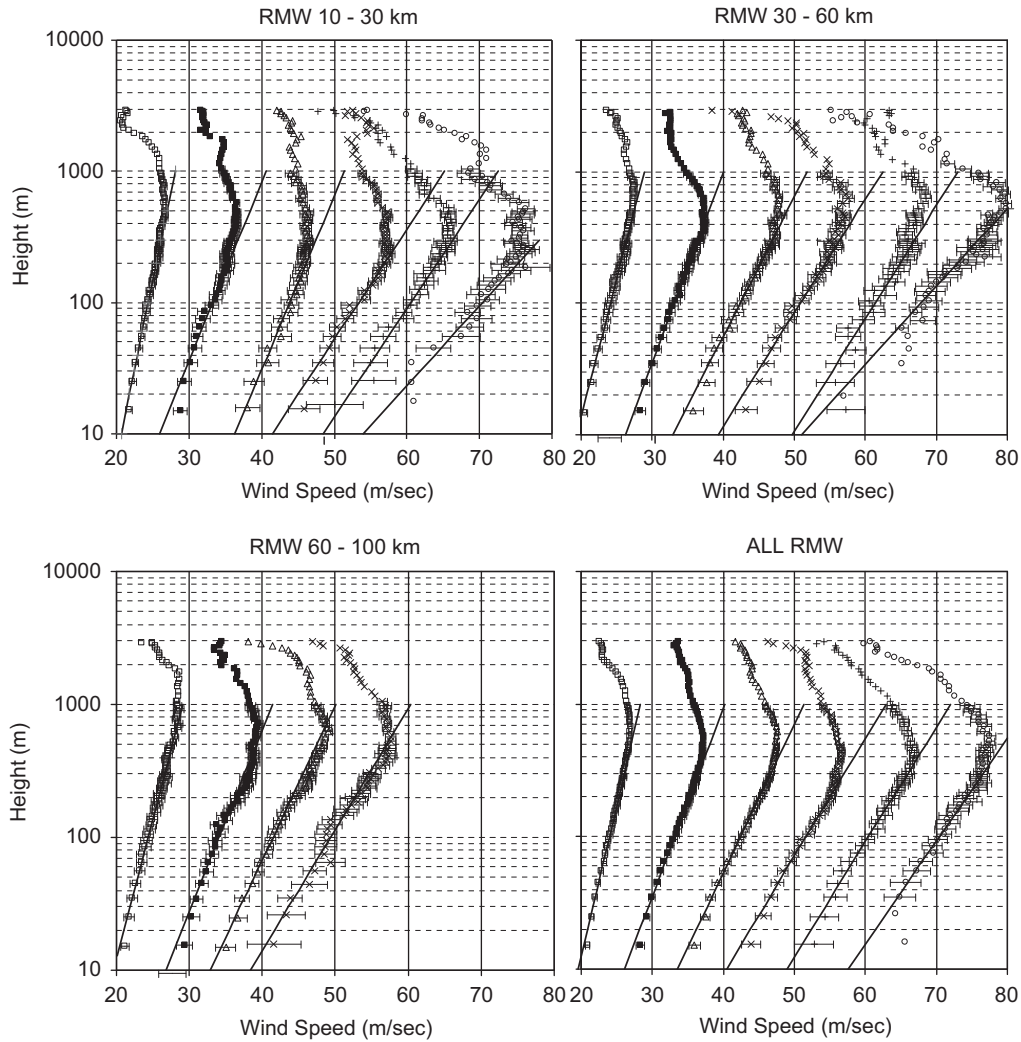


Fig. 2. Mean and fitted logarithmic profiles for drops near the RMW for all MBL cases. Horizontal error bars represent the 95th percentile error on the estimate of the mean wind speed. LSF fits are for the 20–200 m case. (MBL cases correspond to 20–29, 30–39, 40–49, 50–59, 60–69, and 70–85 m/s) (from Vickery et al., 2009b).

Vickery et al. (2009b). All profiles shown in Fig. 2 were taken at or near the RMW.

Vickery et al. (2009b) empirically modeled the variation of the mean wind speed, $U(z)$ with height, z , in the hurricane boundary layer using

$$U(z) = \frac{u_*}{k} \left[\ln\left(\frac{z}{z_0}\right) - 0.4 \left(\frac{z}{H^*}\right)^2 \right] \quad (5)$$

where k is the von-Karman coefficient having a value of 0.4, u_* is the friction velocity, z_0 is the aerodynamic roughness length, and H^* is a boundary layer height parameter that decreases with increasing inertial stability according to

$$H^* = 343.7 + 0.260/I \quad (6)$$

where the inertial stability I is defined as

$$I = \sqrt{\left(f + \frac{2V}{r}\right) \left(f + \frac{V}{r} + \frac{\partial V}{\partial r}\right)} \quad (7)$$

where V is the azimuthally averaged tangential gradient wind speed, f the Coriolis parameter, and r the radial distance from the center of the storm. The boundary layer model described in Vickery et al. (2009b), represents an azimuthally averaged model and ignores the variation in the shape of the hurricane boundary

layer as a function of azimuth in the hurricane as predicted by Kepert (2001).

As in Powell et al. (2003) the sea surface drag coefficient estimated from the dropsondes described in Vickery et al. (2009b) initially increases with wind speed in a fashion similar to that modeled by Large and Pond (1981) and then reaches a maximum value and levels off or decreases (Fig. 3). The mean wind speed at 10 m (U_{10}) at which the sea surface drag coefficient reaches this maximum is only about 25 m/s, (i.e. less than the 40 m/s in Powell et al., 2003) but varied with storm radius. This lower threshold is consistent with the values estimated in Black et al. (2007) of about 23 m/s, although there were limited measurements taken at wind speeds above 25 m/s. The combination of the empirical boundary layer model and the variable cap on the sea surface drag coefficient yield ratios of V_{10}/V_G over the ocean of about 0.67–0.74, varying with both storm size and intensity.

Fig. 4 presents a comparison of the modeled and observed marine wind speed profiles computed using the drag coefficients shown in Fig. 3, and the boundary layer model described by Eqs. (5)–(7), with the only input to the model consisting of the maximum (gradient) wind speed and distance from the center of the storm.

Unfortunately dropsonde data is very limited for velocity profiles over land, and there is thus more reliance on models to

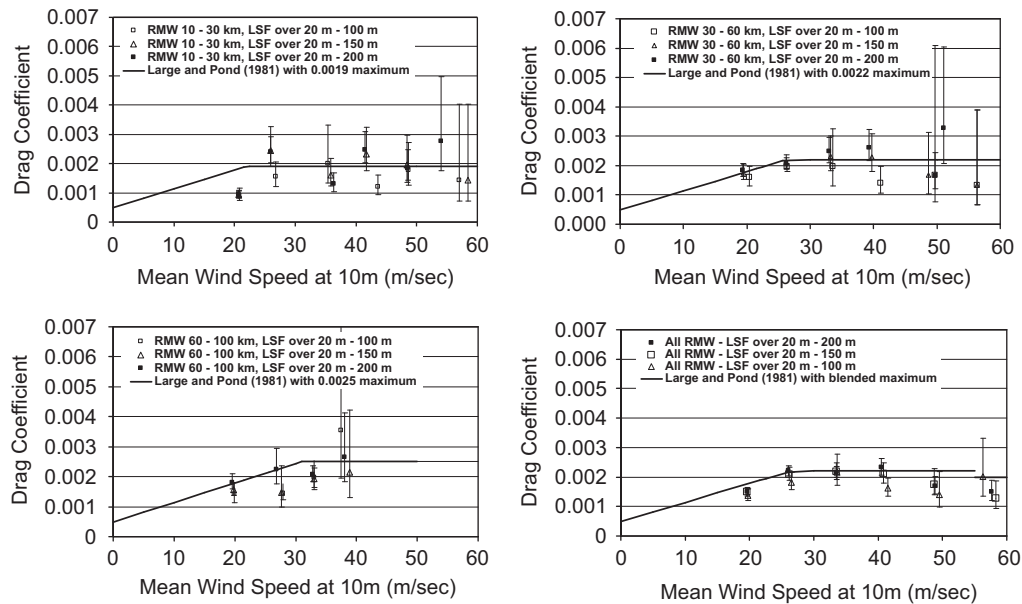


Fig. 3. Variation of the sea surface drag coefficient with U_{10} near the RMW.

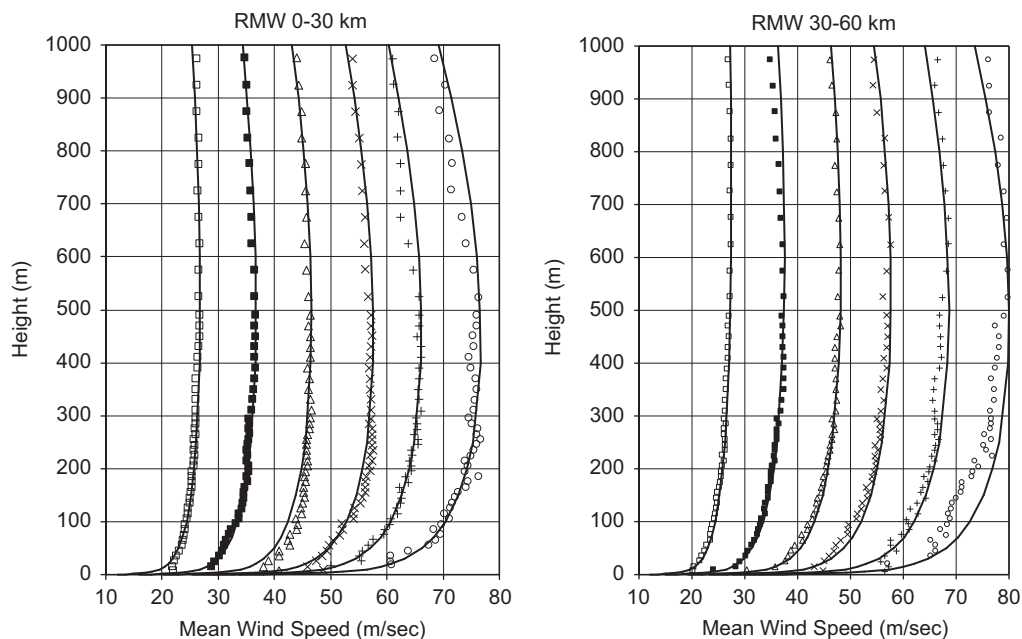


Fig. 4. Modeled and observed hurricane mean velocity profiles over the open ocean for a range of wind speeds.

estimate the characteristics of the hurricane boundary layer over land. The standard engineering approach to modeling terrain change effects is to assume that the wind speed at the top of the boundary layer remains unchanged (but the boundary layer height is free to change), and adjust the winds beneath the BL height to be representative of those associated with the new roughness length. Vickery et al. (2009b), estimated the change in the BL height using Kepert's (2001) linear BL theory, but further increased the BL height increase predicted by Kepert's (2001) model so that the reduction in the surface level winds predicted by the model matched the ESDU values for large BL height. The net result of the Vickery et al. (2009b) approach is estimated BL height increases (from marine to open terrain) in the range of 60–100%, implying overland BL heights in the range of ~800–1500 m depending on wind speed and RMW. Powell et al.

(2005) used a 100% increase in the BL height as the wind transitioned from sea-to-land.

Fig. 5 presents the results of the BL height increase used in Vickery et al. (2009b) as a comparison of the reduction in the surface level winds brought about by the combined effects increased BL height and increased surface roughness as wind transitions from marine to open over land terrain. The upper curve denoted cyclonic flow presents the reduction in the wind speed computed using the Kepert (2001) BL height method, assuming no change in the mean wind speed at the top of the BL.

Once the wind field has been converted from gradient height to 10 m surface level, additional conversions are required to express the influence of varying overland terrain conditions (open, suburban, etc.) as well as averaging times. The common approach is the development and application of gust factors.

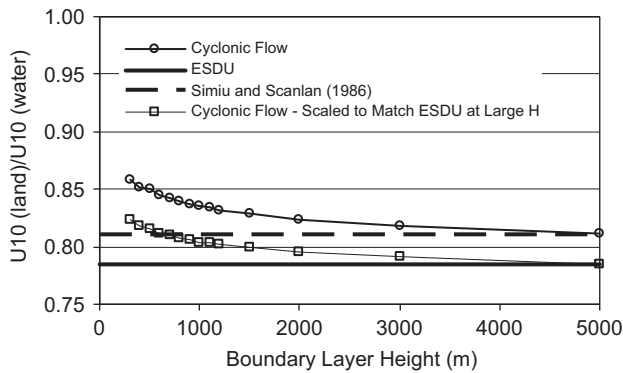


Fig. 5. Ratio of the fully transitioned mean wind speed over land ($z_0 = 0.03$ m) to the mean wind speed over water ($z_0 = 0.0013$ m) as a function of boundary layer height.

3.3. Hurricane gust factors

In many cases, estimates of wind speeds associated with averaging times different to that produced by the basic hurricane wind field model are required in the final application (e.g. 1 min average winds, peak gust wind, etc.). Various representations of a gust factor model for use in hurricanes/tropical cyclones have been employed within different hurricane hazard models. [Batts et al. \(1980\)](#) used the gust factor model described by [Durst \(1960\)](#). [Kramer and Marshall \(1992\)](#) developed a gust factor model for hurricane winds which indicated that the winds associated with hurricanes are “gustier” than those associated with non-hurricanes. [Schroeder et al. \(2002\)](#) and [Schroeder and Smith \(2003\)](#), using wind speed data collected during Hurricane Bonnie, also suggested that hurricane gust factors are larger than those associated with extra-tropical storms.

[Sparks and Huang \(1999\)](#) examined a large number of wind speed records and concluded that there was little evidence to suggest that gust factors associated with hurricanes are different than those associated with extra-tropical storms. [Vickery and Skerlj \(2005\)](#) re-analyzed the data used by [Kramer and Marshall \(1992\)](#) as well as additional data, and concluded that there was no evidence that gust factors associated with hurricanes are different than those associated with extra-tropical storms. [Vickery and Skerlj \(2005\)](#) study further concluded that the mean gust factors in hurricanes could be adequately described using [ESDU \(1982, 1983\)](#) formulations for atmospheric turbulence developed for extra-tropical storms. Both [Sparks and Huang \(1999\)](#) and [Vickery and Skerlj \(2005\)](#) attributed the larger gust factors apparent in [Kramer and Marshall \(1992\)](#) model to surface roughness larger than that typically associated with open terrain (i.e. $z_0 = 0.03$ m). [Miller \(2006\)](#) concurred with the conclusions of [Vickery and Skerlj \(2005\)](#). [Masters \(2005\)](#) presented an analysis of an extensive database of 10 m overland measurements of many US landfalling hurricanes. The significant findings of this analysis included strong evidence that there was no difference between hurricane gust factors and those developed using non-hurricane winds. [Fig. 6](#) presents a comparison of the gust factors (with respect to a 60 s averaging time wind speed) derived from the ESDU model to those presented by [Masters \(2005\)](#), suggesting that the mean gust factors associated with hurricanes are comparable to those predicted using the ESDU models.

The wind speed records obtained in hurricanes suggest that for the most part, the near surface gust factors in hurricanes are similar to those in non-hurricanes. However, there is evidence that there are additional sources of turbulence that may contribute to infrequent and relatively small scale strong winds

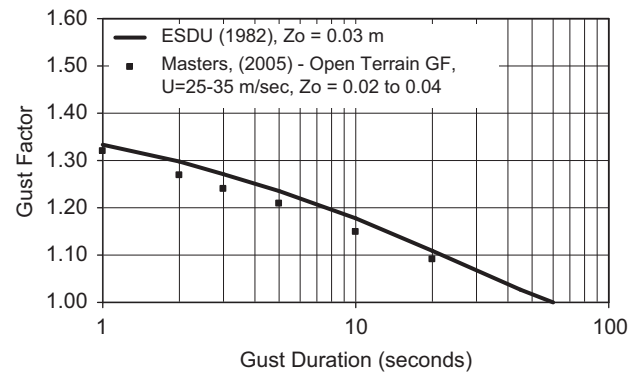


Fig. 6. Comparison of the ESDU gust factor model to those derived from hurricane winds as reported in [Masters \(2005\)](#).

that are much larger than would be predicted by the ESDU gust factor model. These anomalous gusts may be associated with wind swirls generated by horizontal shear vorticity on the inner edge of the eyewall ([Powell and Houston, 1996](#)), coherent linear features e.g. rolls in the boundary layer ([Wurman and Winslow, 1998](#); [Foster, 2005](#)), or other convective features of the storms. While it appears that the ESDU gust factor model provides an adequate description of the gust factors associated with hurricane winds near the surface, additional research is needed to enable modeling of other small scale, but potentially important meteorological phenomena.

3.4. Wind field model validation

An important step in the hurricane risk modeling process is the ability of the wind field model used in the simulation procedure to reproduce wind speeds physically measured in the field. [Georgiou \(1985\)](#) was probably the first to attempt to validate a hurricane wind field model used in a simulation model, looking at the time variation of both wind speeds and wind directions. [Vickery and Twisdale \(1995b\)](#) and [Vickery et al. \(2000a\)](#) performed similar validation analyses and extended the comparisons of wind speed to examine both the mean and gust wind speeds. Similar but limited validation studies for models to be used for hurricane risk assessment have been presented ([Harper, 1999](#); [Lee and Rosowsky, 2007](#)). In [Vickery et al. \(2009b\)](#) comparisons are given for wind speeds, wind directions, and surface pressures, ensuring that the wind model is able to reproduce the observed winds without compromising the ability to model the pressure field. [Fig. 7](#) presents an example of comparisons of modeled and observed wind speeds showing pressures, gust, and average wind speeds, and wind directions. [McConochie et al. \(2004\)](#) also performed validation studies comparing both pressures and wind speeds, but otherwise, pressure verification has not been included in any other model verification studies in the literature.

The wind field model comparisons are important to identify any biases in the wind model portion of the simulation process, but good validations can be a result of other errors that compensate. For example, the high gust factors associated with the use of the Kramer–Marshall gust factors used by [Vickery and Twisdale \(1995b\)](#) partially compensated for an overall underestimate of the mean wind speed at the surface. Similarly, when the hurricane wind models are validated, the validation process is performed using surface level winds, though the basic input to the wind field model is nominally a gradient level wind. Verification of surface winds does not constitute a verification of the upper level winds. This distinction regarding the height at which the validation is performed may be important in

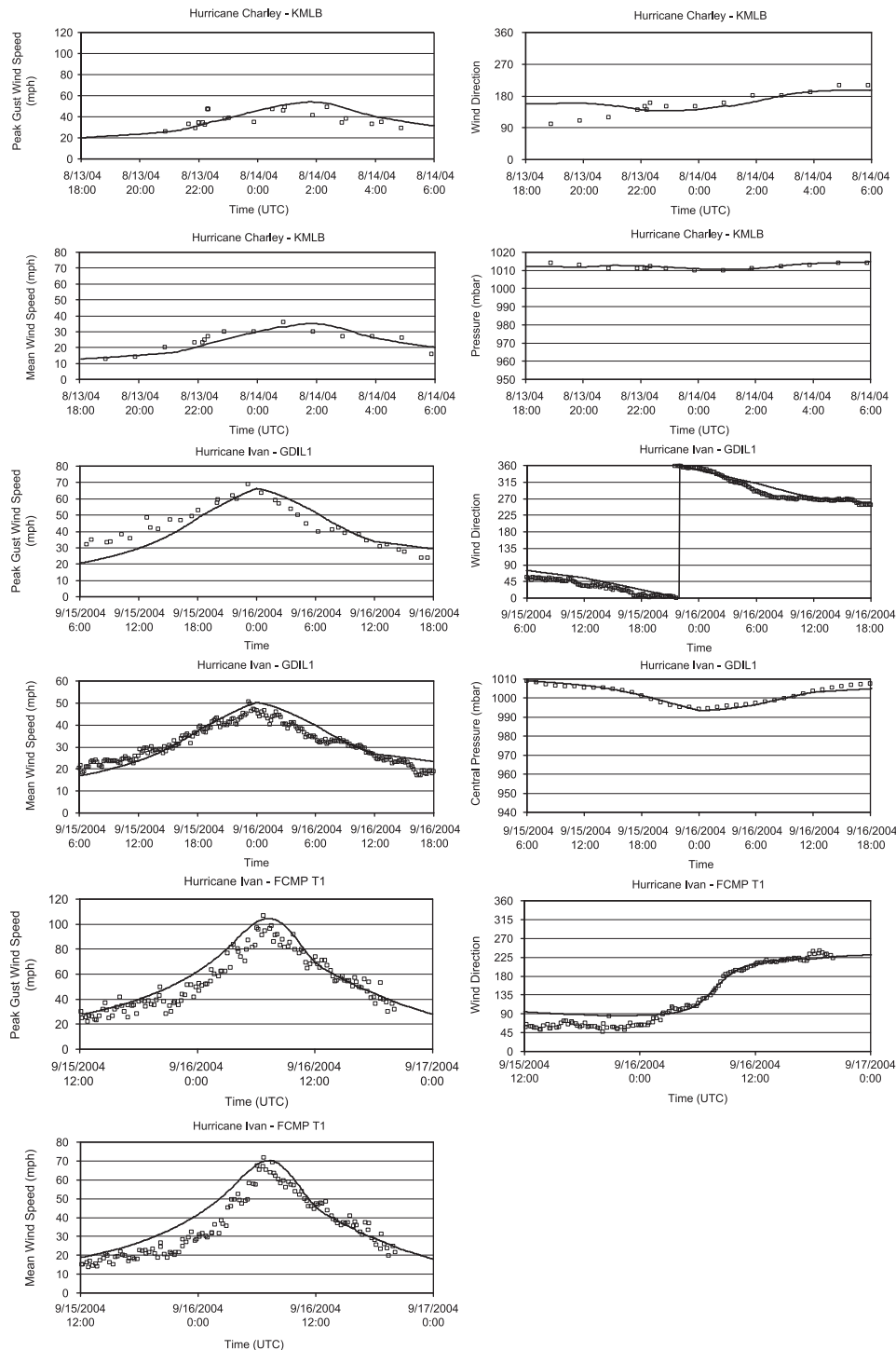


Fig. 7. Example comparisons of model and observed wind speeds, directions and pressures (FCMP = Florida coastal monitoring program, KMLB = Melbourne, Florida ASOS anemometer, GDIL1 = National data Buoy center fixed platform anemometer).

cases where the hurricane simulation results are used in combination with wind tunnel test data for high rise buildings. In both Georgiou (1985) and Vickery and Twisdale (1995a, 1995b), the use of a Holland B parameter of unity coupled with the Shapiro model is now known to yield an underestimate of the gradient wind speed. The underestimate was compensated for by a boundary layer model that was too shallow (i.e. ratios of V_{10}/V_G that were too high), resulting in reasonable estimates of the surface level wind speeds, and underestimates of gradient level wind speeds.

Fig. 8 presents a summary comparison of the maximum peak gust wind speeds computed using the wind field model described in Vickery et al. (2009b) to observations for both marine- and land-based anemometers. There are a total of 245 comparisons summarized in data presented in Fig. 8 (165 land-based measurements and 80 marine-based measurements). The agreement between the model and observed wind speeds is good, however there are relatively few measured gust wind speeds greater than 45 m/s (100 mph). The largest observed gust wind speed is only 57 m/s (128 mph). The differences between the

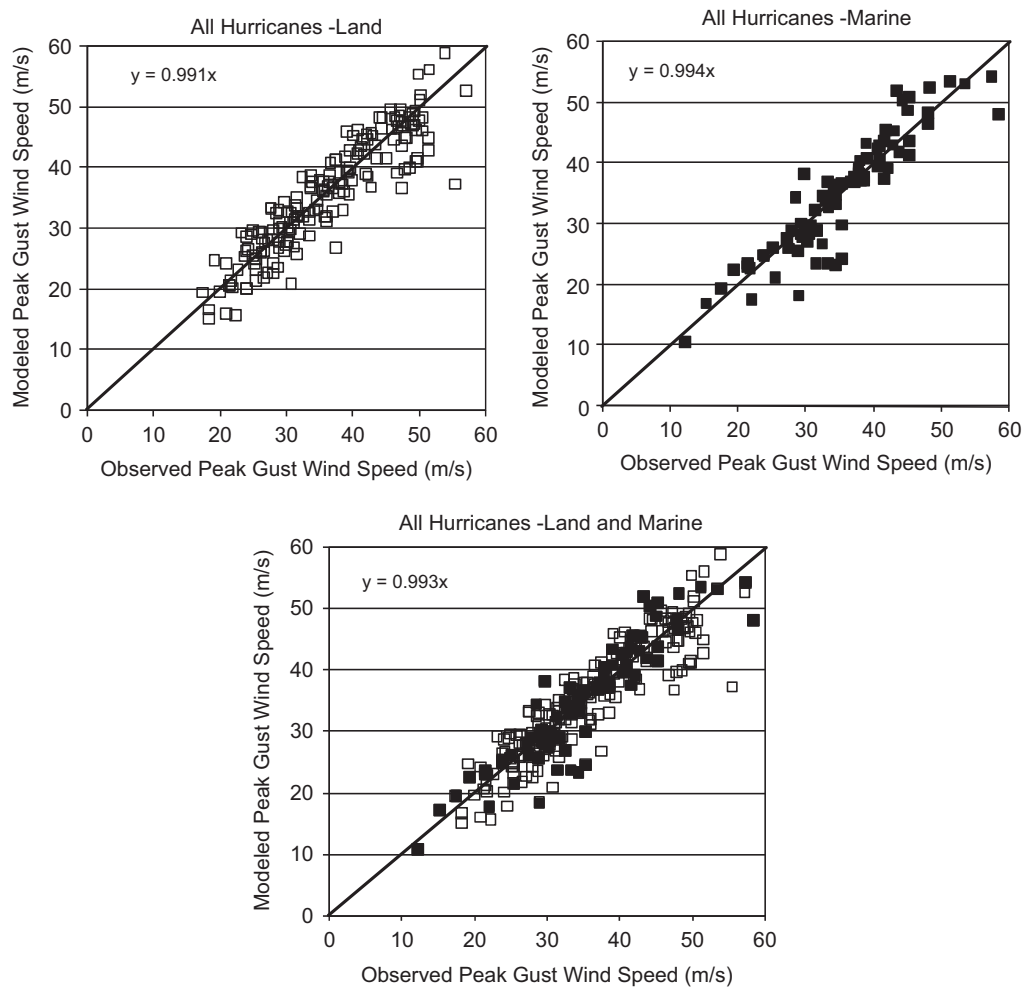


Fig. 8. Example comparisons of modeled and predicted maximum surface level peak gust wind speeds in open terrain from US landfalling hurricanes. Wind speeds measured on land are given for open terrain (open squares) and wind speeds measured over water are given for marine terrain (filled squares).

modeled and observed wind speeds is caused by a combination of the inability of wind field model to be adequately described by a single value of B and RMW , errors in the modeled boundary layer, errors in height, terrain and averaging time adjustments applied to measured wind speeds (if required) as well as storm track position errors and errors in the estimated values of Δp , RMW , and B . The model-observed error information gleaned from the comparisons does provide information required to assess the overall uncertainty of the simulation process, but does not pinpoint the source(s) of error that are worthy of further refinement.

An alternative method of validation is to compare the entire modeled wind field “snapshot” at a particular time to a gridded output from an objective analysis of all available observations over a relatively short (4–6 h) period during which stationarity is assumed. Such analyses are the products of the Hurricane Wind Analysis System (H^* Wind, Powell et al., 1998). An archive of H^* Wind analyses are available at: http://www.aoml.noaa.gov/hrd/data_sub/wind.html. Several examples wind model to H^* Wind comparisons are given in Fig. 9.

The H^* Wind wind field analysis product may be used to derive an estimate of the “observed” Holland B parameter to use in a model. This may be diagnosed by subtracting the storm motion, computing the axi-symmetric radial profile of the surface wind speed, dividing by a gradient to surface wind reduction factor to get a gradient wind estimate, and finally fitting various values of B until the peak gradient wind is matched.

A series of such snapshots may then be combined to construct a “swath” of maximum winds over a gridded domain, an example of which may be found at www.aoml.noaa.gov/hrd/Storm_pages/katrina2005/wind.html. The Florida public hurricane loss model (Powell et al., 2005) incorporates both snapshot and swath comparisons for the validation process. The grid point comparisons are conducted for all points in which the model winds are above wind damage threshold speeds (gust wind speed of ~ 55 mph). While the shapes of the modeled and observed fields have similar features, it is noted that the extent of damaging winds can vary considerably between the fields. Such analyses are especially helpful for identifying biases in the choice of the correct Holland parameter. However, even a B parameter diagnosed from the observations may not be enough to overcome limitations in the Holland pressure profile (Willoughby and Rahn, 2004; Willoughby et al., 2006).

4. Other important model components

Other modeling components important to the overall simulation procedure include the modeling of the radius to maximum winds, the Holland B parameter (for some models) and modeling the weakening of the hurricanes after they make landfall. As demonstrated in Eq. (4), the Holland B parameter plays as important a role in the estimation of the maximum wind speeds, as does Δp . According to Holland (1980), B can vary from about 0.5

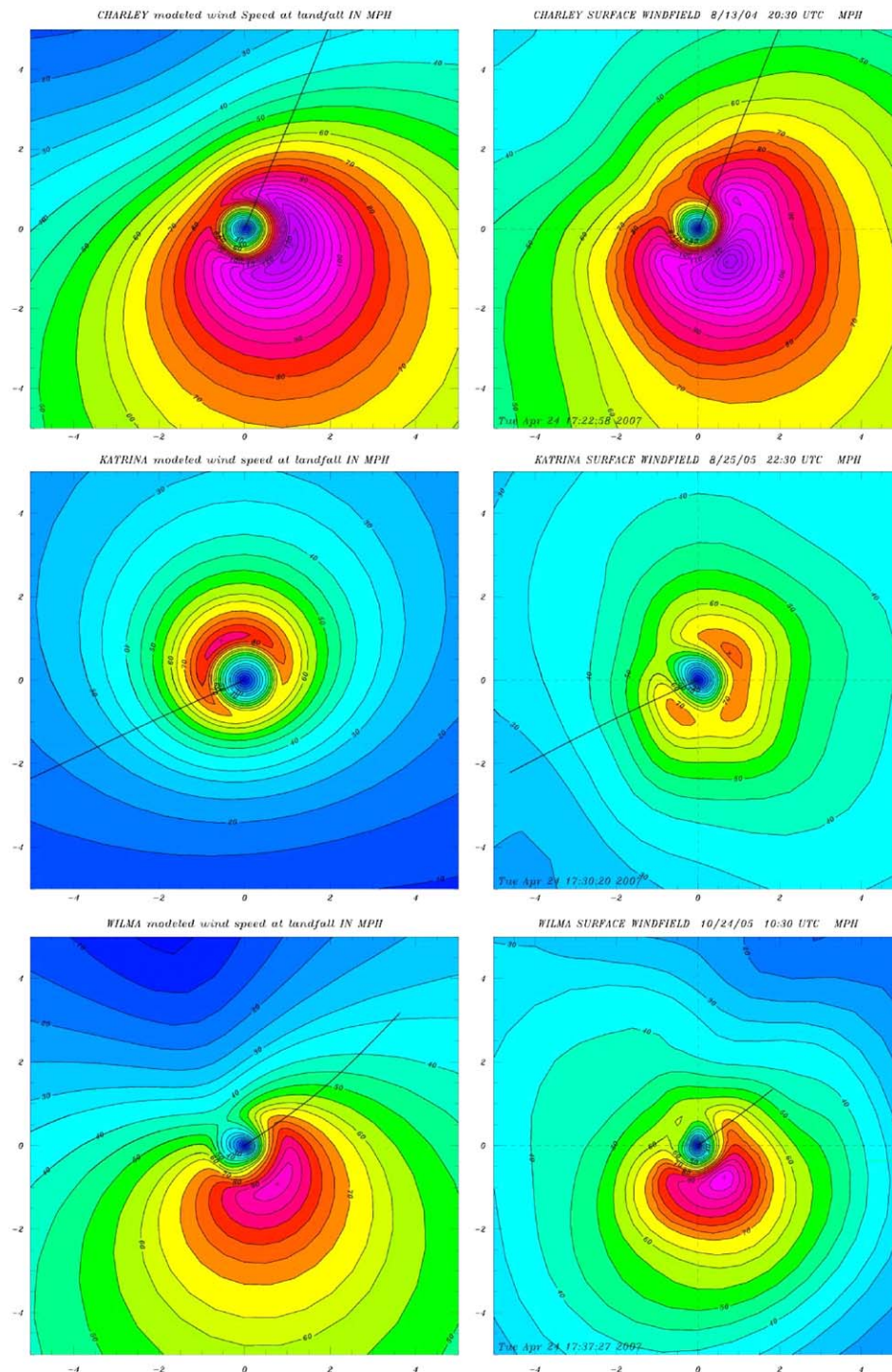


Fig. 9. Comparison of observed (right) and FPHLM modeled (left) landfall wind fields of Hurricanes Charley (2004, top) and 2005, Hurricane Katrina in South Florida (middle), and Hurricane Wilma (bottom). Line segment indicates storm heading. Horizontal coordinates are in units of r/RMW . Winds are for marine exposure.

to about 2.5, however; variations in the range of about 0.7–2.2 (Willoughby and Rahn, 2004; Powell et al., 2005; Vickery and Wadhera, 2008) are more typical and reasonable. Modeling the variation of B has become an important part of the hurricane simulation process, affecting both the magnitude of the maximum wind speeds and the aerial extent over which these large winds extend.

The RMW has no effect on the magnitude of the maximum wind speeds (all else being equal). However, the RMW has a significant influence on the area affected by a storm. For a single

site wind risk study, the modeling of the RMW impacts the likelihood of the site experiencing strong winds in cases of near misses. Modeling of the RMW is critical to storm surge and wave modeling as well as estimating probable maximum losses for insurance modeling purposes. It is generally accepted that the magnitude of the RMW is negatively correlated with the central pressure difference, so that more intense storms (larger central pressure difference) have smaller RMW than the weaker storms. The RMW also increases with increasing latitude. In most models, the RMW is modeled as log-normally distributed with the median

value as function of central pressure and/or latitude. There is significant scatter of field data about the modeled RMW – Δp relationships.

4.1. Statistical model for Holland B parameter

The Holland B parameter can play an important role in the estimation of the maximum wind speeds in a hurricane. Harper and Holland (1999) indicate that for Australian Cyclones, B is a linear function of central pressure, modeled as

$$B = 2.0 - (p_c - 900)/160 \quad (8)$$

so that as the central pressure, p_c , decreases (i.e. Δp increases), B increases.

Vickery et al. (2000a) found a very weak relationship between B and both RMW and Δp , with B decreasing with increasing RMW and increasing with increasing Δp .

Powell et al. (2005), used the values of B computed by Willoughby and Rahn (2004) and flight level data of wind speeds to model the Holland B parameter as a function RMW and latitude, ψ , as

$$B = 1.881 - 0.00557RMW - 0.01097\psi, r^2 = 0.200, \sigma_B = 0.286 \quad (9)$$

where RMW is in km and ψ the latitude expressed as degrees North. Powell et al. (2005) found no relationship between B and central pressure.

Vickery and Wadhera (2008) used the same flight level data as used by Willoughby and Rahn (2004), Willoughby et al. (2006), but fit the radial pressure profiles rather than radial profiles of velocity. Vickery and Wadhera (2008) found that B could be modeled as a function of a non-dimensional parameter, A , shown in Fig. 10 and defined as

$$A = \frac{RMW \cdot f}{\sqrt{2R_d T_s \cdot \ln\left(1 + \frac{\Delta p}{p_c \cdot e}\right)}} \quad (10)$$

The numerator is the product of the RMW (in m) and f , and represents the contribution to angular velocity associated with the Coriolis force. The denominator is an estimate of the maximum potential intensity (as defined by wind speed) of a hurricane. In Eq. (10), R_d is the gas constant for dry air, p_c the central pressure, T_s the sea surface temperature in K. Both the numerator and denominator of A have the units of velocity.

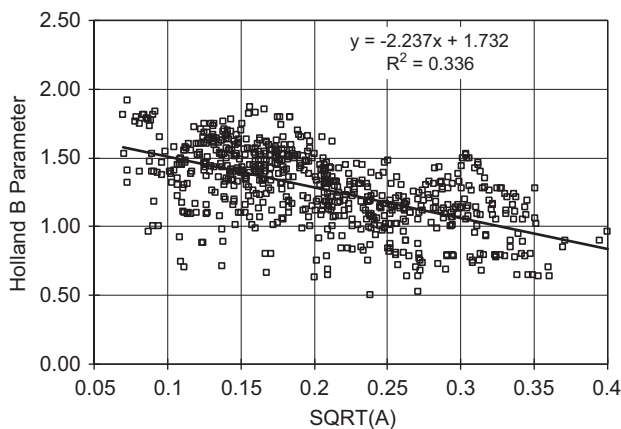


Fig. 10. Relationship between the Holland B parameter and dimensionless parameter, A .

The relationship between B and A is expressed as

$$B = 1.732 - 2.237\sqrt{A}, r^2 = 0.336, \sigma_B = 0.225 \quad (11)$$

Both Powell et al. (2005) and Vickery and Wadhera (2008) found that B decreases with increasing RMW and increasing latitude, and is weakly (if at all) dependent on the central pressure, in contrast to the relationship suggested by Harper and Holland (1999).

The inclusion of modeling B in the simulation process is a significant improvement over the use of a single and constant value of B (usually unity (1) for Atlantic storms). As discussed in Willoughby and Rahn (2004), Willoughby et al. (2006) and Thompson and Cardone (1996), a single value of B cannot model all storms at all times. The simple single parameter model is unable to reproduce the wind fields associated with eyewall replacement cycles, and also has a tendency to underestimate winds speeds well away from the center of the storm. Fortunately, as indicated indirectly in the comparison of modeled and observed wind speeds shown in Figs. 7 and 8, modeling hurricanes with a single value of B is satisfactory in many cases. Hurricane Wilma in South Florida (2005) is an example of a landfalling hurricane that is poorly modeled using a single value of B . Wind speed comparisons for hurricane Wilma are included in those given in Fig. 8. Both surface level anemometer data and remotely sensed data indicate that the strongest surface level winds occurred on the left side of the storm rather than the right as is estimated by modeling the storm with an axi-symmetric pressure field modeled with single values of B and RMW .

4.2. Filling models

Once storms make landfall, they fill or weaken as the central pressure increases. This filling is not to be confused with the additional reduction in wind speeds associated with the increased land friction. Accurate estimates of filling are important for estimating wind speeds at locations removed from the coast by as little as tens of km, and becomes even more important as the distance inland increases. The rate of filling varies with geography, local topography, local climatology, and individual cyclone characteristics. Statistically based filling models should not be applied to regions outside those used to develop the models.

Most filling models (e.g. Batts et al., 1980; Vickery and Twisdale, 1995b; Kaplan and DeMaria, 1995) weaken the storms as a function of time since landfall. A typical filling model is given in the form:

$$\Delta p(t) = \Delta p_0 \exp(-at) \quad (12)$$

where $\Delta p(t)$ is the central pressure difference, t hours after landfall, Δp_0 the central pressure difference at the time of landfall, and a the empirically derived decay constant.

Georgiou (1985) departed from this approach and weaken the storms as a function of distance since landfall. Vickery (2005), revisited the filling of storms impacting the coastal US and found that the rate of filling is best modeled with the decay constant, a , modeled as function of $c\Delta p_0/RMW$, where c is the translation speed of the hurricane at landfall, and Δp_0 the central pressure difference at landfall. The dependence of the filling rate on translation speed at the time of landfall is in general agreement with the findings of Georgiou (1985) who suggested that distance inland is a better indicator of filling than time since landfall.

5. Modeling uncertainty

An assessment of the errors associated with the hurricane simulation process has received very little attention in literature, and even when estimates of the potential errors are presented,

they are typically not used. Batts et al. (1980) carried out a rough error analysis through a combination of sensitivities studies and judgment and suggested that the confidence bounds (\pm one standard deviation) of their predicted wind speeds were about 10% (independent of return period). Twisdale and Vickery (1993) performed an uncertainty study for predicted wind speeds in the Miami area and found a comparable uncertainty.

Vickery et al. (2009a) used a two loop simulation to estimate uncertainty. In this two loop process, the outer loop represents a re-sampling of the parameters defining the statistical distributions used within the N -year simulation. Using this two loop process, they repeated a 100,000 year simulation (inner loop) 5,000 times (outer loop). For each new 100,000 year realization, fully correlated errors in the statistical distributions of landfall central pressure, Holland B parameter and occurrence rate are sampled, and used to perturb these key input variables. Within the inner loop an un-correlated wind field modeling error term (derived from Fig. 8), having a mean of zero and a coefficient of variation of 10% is added to the wind speed computed from the wind field model. The outer loop uncertainty results in a coefficient of variation of the estimated 100 year return period wind speed of about 6%, along the Gulf of Mexico coastline, increasing to about 15% near Maine. The uncertainty in the wind model (treated here as uncorrelated) appears as a shift in the mean wind speed vs. return period curve, rather than appearing as an additional component of the uncertainty in the N -year wind speed.

Fig. 11 presents an example of the estimated uncertainty in the 100 year return period wind speed along the coast of the US, as well as an example of the impact of the wind field model uncertainty on the mean estimate of the N -year return period wind speed. Note that the uncertainty examples given here are representative wind speeds associated with US landfalling hurricanes and would not be representative of the uncertainties in other countries. For example, the landfall pressures for most US landfalling storms have been carefully reconstructed over a 107 year period using combinations of surface and aircraft measurements of pressure, whereas, the Northwest pacific typhoon database is comprised of a combination of aircraft and satellite estimated pressures, which are subject to large and potentially time varying uncertain errors, and covering a much shorter time span.

6. Historical record, climate change, and long period oscillations

Long term trends in the frequency and intensity of tropical cyclones will impact the accuracy of hurricane model-based

products. For example, ASCE design wind speed maps are based upon annualized probabilities of exceedance of peak gust thresholds (N -year recurrence intervals), and these thresholds (model output) will certainly change if intensity and/or frequency trends increase or decrease over the many-year time span used in the model to generate those probabilities. The effects of annual to multi-year (El Niño/La Niña) and multi-decadal oscillations (AMO) are generally accepted, owing to the fact that basin-wide tropical cyclone track and intensity databases (e.g. HURDAT) in the Atlantic and Pacific oceans span multiple cycles of the phenomenon.

There are also varying positions on the existence of longer term trends, as well as their potential causes (natural vs. human influenced). Hurricane models have been used in an attempt to predict the effects of increased atmospheric CO_2 , with no definitive agreement among studies (e.g. Knutson and Tuleya, 2004; Webster et al., 2005). Studies that find a link between sea surface temperatures and hurricane power dissipation (Emanuel, 2005) draw conclusions that are being scrutinized based on the accuracy of the historical data set used in the study. Landsea et al. (2006) and Landsea (2007) re-analyzed satellite imagery and identified as many as 70 previously unrecognized category 4 and 5 cyclones just in the period 1978–1990. These studies conclude that the existing tropical cyclone database is thus unreliable in the detection of trends in the frequency of extreme cyclones.

As the various debates continue on the future and its causes, the science of hurricane wind modeling will need to adapt to future climate trends.

7. Numerical weather prediction models

As previously discussed, the first published hurricane risk model incorporating a numerical weather prediction type of model is that of Emanuel et al. (2006), which coupled Emanuel's CHIPS (coupled hurricane intensity prediction system) hurricane intensity model with the NCAR climate re-analysis data. Two different versions of the hurricane risk model were developed, and both versions use a deterministic 1-D numerical hurricane intensity model (Emanuel et al., 2004), a simple ocean feedback model, and a statistically based wind shear model. Two different track models were developed, one using a Markov modeling approach similar to that of Vickery et al. (2000b) and the other modeling the hurricane track using a weighted average of an environmental flow as a track predictor, also derived from the NCAR re-analysis data. The model was validated through comparisons of model estimated maximum winds with NHC best track data. No validation of storm size was presented, nor was the

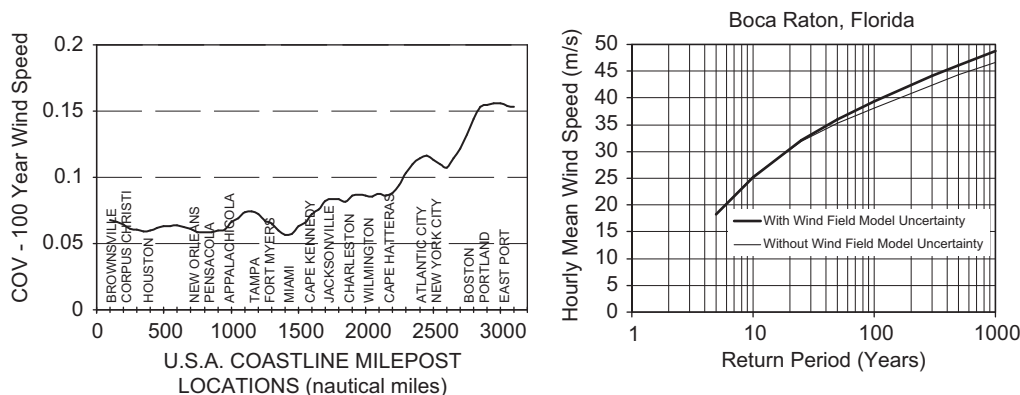


Fig. 11. Estimate coefficient of variation (smoothed) of the 100 year return period wind speed along the coastline of the US (left plot) and effect of windfield modeling uncertainty of the predicted wind speed vs. return period for a single location.

wind model validated with comparisons with surface level anemometer data or H^* Wind data.

Similar approaches have been taken by others using the GFDL model, MM5, and the WRF model, however; results have not been published in the peer reviewed literature, and therefore it is impossible to determine the validity of the approaches. Modeling hurricane risk with NWP models reduces, to an extent, the need to rely on statistical models, however; as noted in Chen et al. (2007), the model results are sensitive to modeling details, such as the modeling of the sea surface drag coefficient, boundary layer parameterization, grid resolution (both horizontal and vertical), and factors that affect surface heat flux modeling such as sea spray, etc.

To be useful in hurricane risk assessment studies, the NWP models will have to be validated both through comparisons of modeled and observed wind speeds for historical storms using only parameters that are used in the stochastic model version. The stochastic versions of the NWP models must also be able to reasonably well reproduce observed historical landfall rates, $RMW-\Delta p$ relationships, storm weakening characteristics, etc. NWP models are likely to be used in the next generation of hurricane risk models, but it remains to be seen, at least in the short term, what improvements will be made in terms of reducing the overall modeling uncertainty.

8. Summary

Hurricane hazard models provide data that drives wind tunnel and risk modeling for a wide range of applications, including insurance loss estimation, prescription of design wind loading, and prediction/reconstruction of catastrophic hurricane wind fields. The basis of most models are parametric track and intensity projections that provide gradient wind speeds, which are adjusted to site-specific terrain and desired gust-averaging periods. Inland decay is also considered once the storm transitions onto land. Sensitivity studies have shown that uncertainty in the N -year return period wind speed estimate is of the order of $\sim 10\%$ along the US coastline. A critical step in the modeling process is the validation of the outputs, which are compared to climatological or event specific wind speed and barometric pressure data and estimations from land-, marine-, aircraft-, and satellite-based observing platforms.

Hurricane hazard modeling has evolved significantly since its origin in the late 1960s. Regarding the future, next generation models may incorporate the effects of climate change and utilize advancements in numerical weather prediction. It is debatable how advances in our understanding of climate change will alter current modeling practice, however. Tropical meteorology and climatologists have not reached a consensus opinion on the effect of long-term trends, owing, in part, to short and often incomplete tropical cyclone databases.

References

- American National Standards Institute, Inc., 1982. Minimum Design Loads for Buildings and Other Structures. ANSI A58.1, New York.
- American Society of Civil Engineers, 1993. ASCE-7 Minimum Design Loads for Buildings and Other Structures. ASCE, New York.
- American Society of Civil Engineers, 2006. ASCE-7 Minimum Design Loads for Buildings and Other Structures. ASCE, New York.
- AS/NZS1170.2, 2002. Standards Australia/Standards New Zealand. Structural design actions, part 2: wind actions, AS/NZS1170.2-2002.
- Batts, M.E., Cordes, M.R., Russell, L.R., Shaver, J.R., Simiu, E., 1980. Hurricane wind speeds in the United States. National Bureau of Standards, Report Number BSS-124, US Department of Commerce, 50pp.
- Black, P.G., D'saro, E.A., Drennan, W.M., French, J.R., Niler, P.P., Sanford, T.B., Terrill, E.J., Walsh, E.J., Zhang, J.U., 2007. Air-sea exchange in hurricanes: synthesis of observations from coupled boundary layer air-sea transfer experiment. Bull. Am. Meteorol. Soc. 89, 357–374.
- Caribbean Uniform Building Code (CUBIC), 1985. Structural design requirements WIND LOAD, part 2, section 2. Caribbean Community Secretariat, Georgetown, Guyana.
- Chen, S.C., Price, J., Zhao, W., Donelan, M.A., Walsh, E.J., 2007. The CBLAST hurricane program and the next generation fully coupled atmosphere-wave-ocean models for hurricane research and prediction. Bull. Am. Meteorol. Soc. 88, 311–317.
- Darling, R.W.R., 1991. Estimating probabilities of hurricane wind speeds using a large-scale empirical model. J. Climate 4, 1035–1046.
- DeMaria, M., Knaff, J.A., Kaplan, J., 2006. On the decay of tropical cyclone winds crossing narrow landmasses. J. Appl. Meteorol. 45, 491–499.
- Durst, C.S., 1960. Wind speeds over short periods of time. Meteorol. Mag. 89, 181–186.
- Emanuel, K.A., 2005. Increasing destructiveness of tropical cyclones over the past 30 years. Nature 436, 686–688.
- Emanuel, K.A., 1988. The maximum intensity of hurricanes. J. Atmos. Sci. 45, 1143–1155.
- Emanuel, K.A., DesAutels, C., Holloway, C., Korty, R., 2004. Environmental control of tropical cyclone intensity. J. Atmos. Sci. 61, 843–858.
- Emanuel, K.A., Ravela, S., Vivant, E., Risi, C., 2006. A statistical-deterministic approach to hurricane risk assessment. Bull. Am. Meteorol. Soc. 19, 299–314.
- ESDU, 1982. Strong winds in the atmospheric boundary layer, part 1: mean hourly wind speed. Engineering Sciences Data Unit Item No. 82026, London, England.
- ESDU, 1983. Strong winds in the atmospheric boundary layer, part 2: discrete gust speeds. Engineering Sciences Data Unit Item No. 83045, London, England.
- Foster, R.C., 2005. Why rolls are prevalent in the hurricane boundary layer. J. Atmos. Sci. 62, 2647–2661.
- Georgiou, P.N., 1985. Design windspeeds in tropical cyclone-prone regions. Ph.D. Thesis, Faculty of Engineering Science, University of Western Ontario, London, Ontario, Canada.
- Georgiou, P.N., Davenport, A.G., Vickery, B.J., 1983. Design wind speeds in regions dominated by tropical cyclones. J. Wind Eng. Ind. Aerodyn. 13, 139–152.
- Harper, B.A., 1999. Numerical modeling of extreme tropical cyclone winds. J. Ind. Aerodyn. 83, 35–47.
- Harper, B.A., Holland, G.J., 1999. An updated parametric model of tropical cyclone. In: Proceedings of 23rd Conference on Hurricanes and Tropical Meteorology, American Meteorological Society, Dallas, TX.
- Hall, T., Jewson, S., 2005. Statistical modeling of tropical cyclone tracks, part 1–6. arXiv:physics.
- Hall, T., Jewson, S., 2008. Comparison of local and basin-wide methods for risk assessment of tropical cyclone landfall. J. Appl. Meteorol. Climatol. 47, 361–367.
- Holland, G.J., 1980. An analytic model of the wind and pressure profiles in hurricanes. Mon. Weather Rev. 108, 1212–1218.
- James, M.K., Mason, L.B., 2005. Synthetic tropical cyclone database. J. Waterw. Port Coastal Ocean Eng. 131, 181–192.
- Jarvinen, B.R., Neumann, C.J., Davis, M.A.S., 1984. A tropical cyclone data tape for the North Atlantic Basin 1886–1983: contents, limitations and uses. NOAA Technical Memorandum NWS NHC 22, US Department of Commerce, March.
- Kaplan, J., De Maria, M., 1995. A simple empirical model for predicting the decay of tropical cyclone winds after landfall. J. Appl. Meteorol. 34, 2499–2512.
- Keptert, J., 2001. The dynamics of boundary layer jets within the tropical cyclone core. Part I: linear theory. J. Atmos. Sci. 58, 2469–2484.
- Knutson, T.R., Tuleya, R.E., 2004. Impact of CO₂-induced warming on simulated hurricane intensity and precipitation: sensitivity to the choice of climate model and convective parameterization. J. Climate 17, 3477–3495.
- Krayer, W.R., Marshall, R.D., 1992. Gust factors applied to hurricane winds. Bull. Am. Meteorol. Soc. 73, 270–280.
- Landsea, C.W., 2007. Counting Atlantic tropical cyclones back to 1900. Eos Trans. AGU 88, 197–208.
- Landsea, C.W., Harper, B.A., Hoarau, K. Can we detect trends in extreme tropical cyclones? Science 313, 452–454.
- Large, W.G., Pond, S., 1981. Open ocean momentum flux measurements in moderate to strong winds. J. Phys. Oceanogr. 11, 324–336.
- Lee, K.H., Rosowsky, D.V., 2007. Synthetic hurricane wind speed records: development of a database for hazard analyses and risk studies. Nat. Hazards Rev. 8, 23–34.
- Masters, F., 2005. Measurement of tropical cyclone surface winds at landfall. In: 59th Interdepartmental Hurricane Conference, Jacksonville, FL, March 7–11.
- McConochie, J.D., Hardy, T.A., Mason, L.B., 2004. Modeling tropical cyclone over water wind and pressure fields. Ocean Eng. 31, 1757–1782.
- Miller, C.A., 2006. Gust factors in hurricane and non-hurricane conditions. In: 27th Conference on Hurricanes and Tropical Meteorology, American Meteorological Society, Monterey, CA.
- Neumann, C.J., 1991. The National Hurricane Center Risk Analysis Program (HURISK). NOAA Technical Memorandum NWS NHC 38, National Oceanic and Atmospheric Administration (NOAA), Washington, DC.
- Powell, M.D., 2007. Personal communication.
- Powell, M.D., Houston, S.H., 1998. Hurricane Andrew's Landfall in South Florida. Part II: Surface wind fields and potential real-time applications. Weather Forecast. 11, 329–349.
- Powell, M.D., Houston, S.H., Amat, L.R., Morrisseau-Leroy, N., 1998. The HRD real-time hurricane wind analysis system. J. Ind. Aerodyn. 77–78, 53–64.

- Powell, M.D., Soukup, G., Cocke, S., Gulati, S., Morisseau-Leroy, N., Hamid, S., Dorst, N., Axe, L., 2005. State of Florida hurricane loss projection model: atmospheric science component. *J. Ind. Aerodyn.* 93, 651–674.
- Powell, M.D., Vickery, P.J., Reinhold, T.A., 2003. Reduced drag coefficient for high wind speeds in tropical cyclones. *Nature* 422, 279–283.
- Russell, L.R., 1968. Probability distribution for Texas Gulf coast hurricane effects of engineering interest. Ph.D. Thesis, Stanford University.
- Russell, L.R., 1971. Probability distributions for hurricane effects. *J. Waterw., Harbors, Coastal Eng. Div.* 97, 139–154.
- Schwerdt, R.W., Ho, F.P., Watkins, R.W., 1979. Meteorological criteria for standard project hurricane and probable maximum hurricane wind fields, Gulf and East Coasts of the United States. NOAA Technical Report NWS 23, US Department of Commerce, Washington, DC.
- Schroeder, J.L., Smith, D.A., 2003. Hurricane Bonnie wind flow characteristics as determined from WEMITE. *J. Ind. Aerodyn.* 91, 767–789.
- Schroeder, J.L., Conder, M.R., Howard, J.R., 2002. Additional insights into hurricane gust factors. In: 25th Conference on Hurricanes and Tropical Meteorology, San Diego, CA, pp. 39–40 (Pre-prints).
- Shapiro, J.J., 1983. The asymmetric boundary layer under a translating hurricane. *J. Atmos. Sci.* 40, 1984–1998.
- Simiu, E., Scanlan, R.H., 1996. *Wind Effects on Buildings and Structures Fundamentals and Applications to Design*, third ed Wiley-Interscience 688pp.
- Skamarock, W.C., Klemp, J.B., Dudhia, J., Gill, D.O., Barker, D.M., Duda, M., Huang, X.-Y., Wang, W., Powers, J.G., 2008. A description of the advanced research WRF version 3. NCAR Technical Note, NCAR/TN-475+STR, 113pp.
- Sparks, P.R., 2003. Wind speeds in tropical cyclones and associated insurance losses. *J. Wind Eng. Ind. Aerodyn.* 91, 1731–1751.
- Sparks, P.R., Huang, Z., 1999. Wind speed characteristics in tropical cyclones. In: *Proceedings of 10th International Conference on Wind Engineering*, Copenhagen, pp. 343–350.
- Sparks, P.R., Huang, Z., 2001. Gust factors and surface-to-gradient wind speed ratios in tropical cyclones. *J. Ind. Aerodyn.* 89, 1058–1470.
- Thompson, E.F., Cardone, V.J., 1996. Practical modeling of hurricane surface wind fields. *J. Waterw., Port, Coastal, Ocean Eng.* 122, 195–205.
- Tryggvason, V.J., Davenport, A.G., Surry, D., 1976. Predicting wind-induced response in hurricane zones. *J. Struct. Div.* 102, 2333–2350.
- Twisdale, L.A., Vickery, P.J., 1993. Uncertainties in the prediction of hurricane windspeeds. In: *Proceedings of Hurricanes of 1992*, ASCE, December, pp. 706–715.
- Vickery, V.J., Wadhera, D., Twisdale, L.A., Lavelle, F.M., 2009a. United States hurricane wind speed risk and uncertainty. *J. Struct. Eng.* 135, 301–320.
- Vickery, V.J., Wadhera, D., Powell, M.D., Chen, Y., 2009b. PA hurricane boundary layer and wind field model for use in engineering applications. *J. Appl. Meteorol.* 48, 381–405.
- Vickery, P.J., Wadhera, D., 2008. Statistical models of Holland pressure profile parameter and radius to maximum winds of hurricanes from flight level pressure and *H*Wind* data. *J. Appl. Meteorol.* 47, 2417–2497.
- Vickery, P.J., 2005. Simple empirical models for estimating the increase in the central pressure of tropical cyclones after landfall along the coastline of the United States. *J. Appl. Meteorol.* 44, 1807–1826.
- Vickery, P.J., Skerlj, P.F., 2005. Hurricane gust factors revisited. *J. Struct. Eng.* 131, 828–832.
- Vickery, P.J., Skerlj, P.F., Steckley, A.C., Twisdale Jr., L.A., 2000a. Hurricane wind field model for use in hurricane simulations. *J. Struct. Eng.* 126 (10), 1203–1221.
- Vickery, P.J., Skerlj, P.F., Twisdale Jr., L.A., 2000b. Simulation of hurricane risk in the US using an empirical track model. *J. Struct. Eng.* 126 (10), 1222–1237.
- Vickery, P.J., Twisdale Jr., L.A., 1995a. Prediction of hurricane wind speeds in the US. *J. Struct. Eng.* 121, 1691–1699.
- Vickery, P.J., Twisdale Jr., L.A., 1995b. Wind field and filling models for hurricane wind speed predictions. *J. Struct. Eng.* 121, 1700–1709.
- Warner, T.T., Anthes, R.A., McNab, A.L., 1978. Numerical simulations with a three dimensional mesoscale model. *Mon. Weather Rev.* 106, 1079–1099.
- Webster, P.J., Holland, G.J., Curry, J.A., Chang, H.-R., 2005. Changes in tropical cyclone number, duration, and intensity in a warming environment. *Science* 309, 1844–1846.
- Willoughby, H.E., Rahn, M.E., 2004. Parametric representation of the primary hurricane vortex. Part I: observations and evaluation of the Holland (1980) model. *Mon. Weather Rev.* 132, 3033–3048.
- Willoughby, H.E., Darling, R.W.R., Rahn, M.E., 2006. Parametric representation of the primary hurricane vortex. Part II: a new family of sectional continuous profiles. *Mon. Weather Rev.* 134, 1102–1120.
- Wurman, J., Winslow, J., 1998. Intense sub-kilometer-scale boundary layer rolls observed in Hurricane Frances. *Science* 280, 555–557.